Biol. Cell (2012) **104**, 84–101 DOI: 10.1111/boc.201100080

Research article

Rab30 is required for the morphological integrity of the Golgi apparatus

Eoin E. Kelly*, Francesca Giordano†‡‖, Conor P. Horgan*, Florence Jollivet†§, Graça Raposo†‡‖ and Mary W. McCaffrey*[1]

*Molecular Cell Biology Laboratory, Department of Biochemistry, BioSciences Institute, University College Cork, Cork, Ireland, †Institut Curie, Centre de Recherche, Paris F-75248, France, ‡Structure and Membrane Compartments, Centre National de la Recherche Scientifique (CNRS), UMR144, Paris F-75248, France, ‖Cell and Tissue Imaging Facility, Infrastructures en Biologie Sante et Agronomie, Paris F-75248, France, and §Molecular Mechanisms of Intracellular Transport, CNRS, UMR144, Paris F-75248, France

Background information. Rab GTPases are key coordinators of eukaryotic intracellular membrane trafficking. In their active states, Rabs localise to the cytoplasmic face of intracellular compartments where they regulate membrane trafficking processes. Many Rabs have been extensively characterised whereas others, such as Rab30, have to date received relatively little attention.

Results. Here, we demonstrate that Rab30 is primarily associated with the secretory pathway, displaying predominant localisation to the Golgi apparatus. We find by time-lapse microscopy and fluorescence recovery after photobleaching studies that Rab30 is rapidly and continuously recruited to the Golgi. We also show that Rab30 function is required for the morphological integrity of the Golgi. Finally, we demonstrate that inactivation of Rab30 does not impair anterograde or retrograde transport through the Golgi.

Conclusions. Taken together, these data illustrate that Rab30 primarily localises to the Golgi apparatus and is required for the structural integrity of this organelle.

Supporting Information available online

Introduction

The complex endomembrane system of membrane-bound compartments and organelles that exist in eukaryotic cells requires sophisticated mechanisms for the transport of cellular material from one location to another. Such a multifarious trafficking system requires several critical cellular transport events such as vesicle budding and formation, motility, docking and fusion.

Central to the control and regulation of vesicle trafficking is the Rab family of GTPases, the largest subfamily of the small GTPases (Stenmark, 2009). Rab proteins are low-molecular-weight (20–25 kDa) monomeric GTPases that act as cellular molecular switches by alternating between two distinct nucleotide-bound conformations (Stenmark, 2009). When GDP-bound, Rabs are inactive and associate with chaperone proteins termed GDP-dissociation inhibitors (GDIs) which facilitate their extraction from, and delivery to, appropriate membranes. In this functional cycle, once a Rab becomes membrane associated, rapid exchange of GDP for GTP occurs and it switches to its 'active' conformation. The active Rab can recruit downstream effector proteins which mediate its biological function. Following this, the

[1]To whom correspondence should be addressed (email m.mccaffrey@ucc.ie).
Key words: Fluorescence techniques, Golgi, GTPase, Membrane transport, Rab30.
Abbreviations used: BFA, brefeldin A; CTxB, cholera toxin fragment B; EM, electron microscopy; ER, endoplasmic reticulum; ERC, endosomal-recycling compartment; ERGIC, ER–Golgi intermediate compartment; FRAP, fluorescence recovery after photobleaching; FLIP, fluorescence loss in photobleaching; GalT, β1, 4-galactosyltransferase I; GDI, GDP-dissociation inhibitor; GFP, green fluorescent protein; JNK, jun-N-terminal kinase; KDEL-R, (Lys–Asp–Glu–Leu) endoplasmic reticulum protein retention receptor; PM, plasma membrane; PAG, protein A–gold; ROI, region of interest; RT-PCR, reverse-transcription polymerase chain reaction; TGN, *trans*-Golgi network; TfnR, transferrin receptor; VSV-G, vesicular stomatitis virus glycoprotein.

Rab hydrolyses the bound GTP, returning the Rab to its 'inactive' GDP-bound state, which is followed by subsequent membrane extraction by GDI and, when appropriate, delivery of the Rab to a new membrane for another round of functional activity (Stenmark, 2009).

The eukaryotic biosynthetic pathway is composed of the endoplasmic reticulum (ER), the Golgi apparatus and intermediate compartments between these two organelles (Lee et al., 2004). The primary function of these compartments is to correctly fold newly synthesised proteins, to perform essential post-translational modifications, and to package proteins into vesicles for their transportation to a target intracellular destination or to the plasma membrane (PM) (Glick and Nakano, 2009). The trafficking systems that exist between the ER and Golgi are tightly regulated by a collection of small GTPases including Rab1a, Rab1b, Rab2, Arl1 and ARF1 (Lee et al., 2004). These proteins have primarily been implicated in directing the assembly of the COPI and COPII coat complexes that facilitate vesicle budding from donor compartments, and also in the control of vesicle fusion in conjunction with tethering proteins that are anchored in acceptor compartments (Tisdale et al., 1992; Moyer et al., 2001; Lee et al., 2004; Glick and Nakano, 2009). Trafficking from the Golgi to endosomes and to the PM is controlled by a different subset of Rab proteins including Rab6, Rab8, Rab11 and Rab14 (Huber et al., 1993; Chen et al., 1998; Wilcke et al., 2000; Grigoriev et al., 2007; Kitt et al., 2008).

Rab30 is a ubiquitously expressed, 23 kDa GTPase that was first identified from human melanocyte cDNA and mapped to chromosome 11 (Chen et al., 1996). An initial immunoelectron microscopy (IEM) study revealed that epitope-tagged Rab30 is primarily associated with Golgi cisternae in simian COS-1 cells (de Leeuw et al., 1998). Subsequently, Rab30 was shown to associate with a number of golgin proteins in *Drosophilia melanogaster*, namely, dGolgin-245, dGolgin-97, dGM130 and dGCC88 and with the fly orthologues of the coiled-coil proteins p115 and Bicaudal D (BicD) (Sinka et al., 2008). However, the functional significance of these interactions is currently unknown. Recent work has identified Rab30 as a target of the jun-N-terminal kinase (JNK), an important regulator of gene expression (Thomas et al., 2009). Continuous activation of the JNK pathway results in significant upregulation of Rab30 expression (Thomas et al., 2009). Depletion of Rab30 by RNA interference (RNAi) results in defects in dorsal closure, head involution and thorax fusion during *D. melanogaster* development (Thomas et al., 2009). The increased activation of the JNK pathway during development may increase the cellular levels of Rab30, resulting in a consequential increase in the trafficking of material in leading-edge cells which facilitates dorsal closure, head involution and thorax fusion (Thomas et al., 2009). Recent work has also demonstrated that Rab30 is upregulated in polyaromatic hydrocarbon-induced tumourigenesis, suggesting that it may play an important role in the development of certain human cancers (Shi et al., 2010).

Here, through a combination of immunofluorescence, electron and time-lapse microscopy in combination with inactivation studies and trafficking assays, we provide an in-depth analysis of Rab30 localisation, and define a role for Rab30 in maintaining the organisation of the Golgi compartment.

Results

Rab30 is primarily associated with the Golgi

To examine the subcellular distribution of Rab30 in a human cell line, HeLa cells were transfected with GFP–Rab30. We found by confocal immunofluorescence microscopy that Rab30 was primarily associated with a compartment proximal to the nucleus, but also displayed some dispersed reticular staining, with a minor proportion also present in the cytosol (Figure 1A). The GFP–Rab30-positive juxtanuclear compartment stained strongly for GM130, Rab6 and TGN46, markers of the *cis-,* medial- and *trans*-Golgi and *trans*-Golgi network (TGN), respectively (Figure 1A). Extending these observations, immunoelectron microscopy (IEM) on cells expressing FLAG–Rab30 revealed that Rab30 is distributed throughout the Golgi cisternae (Figure 1B). A quantitative evaluation of the distribution of FLAG–Rab30 on ultrathin cryosections of cells that were double immunogold labelled for FLAG–Rab30 and the (Lys–Asp–Glu–Leu) endoplasmic reticulum protein retention receptor (KDEL-R), which cycles between the Golgi and ER, indicated that Rab30 is primarily distributed to the Golgi, TGN and to the cytoplasm with lower proportions in the ER, endosomes and cytoplasmic vesicles (Figures

Figure 1 | Exogenous Rab30 localises to the Golgi apparatus

(**A**) HeLa cells were transfected with pEGFP-C1/Rab30. Sixteen to 18 h after transfection, the cells were processed for immunofluorescence microscopy and immunostained with antibodies to GM130, Rab6 or TGN46. Scale bar indicates 10 μm. (**B**) Ultrathin cryosections of HeLa cells expressing a Rab30-Flag construct were double immunogold labelled with an anti-Flag antibody (PAG15) and an anti-KDEL-R antibody (PAG10). Arrows and inset indicate vesicles, some of which are labelled for FLAG–Rab30 and the KDEL-R (arrows and inset). Scale bar indicates 0.4 μm. (**C**) Quantification of the labelling for Rab30 on ultrathin cryosections of HeLa cells. Results are presented as the percentage of the total number of gold particles for Rab30 in the morphologically distinct compartments (mean $\pm$SD). GA, Golgi apparatus; TGN, *trans*-Golgi network; End, endosome; ER, endoplasmic reticulum; Ves, vesicles; CF, cytosolic fraction. All data are typical of at least three independent experiments.

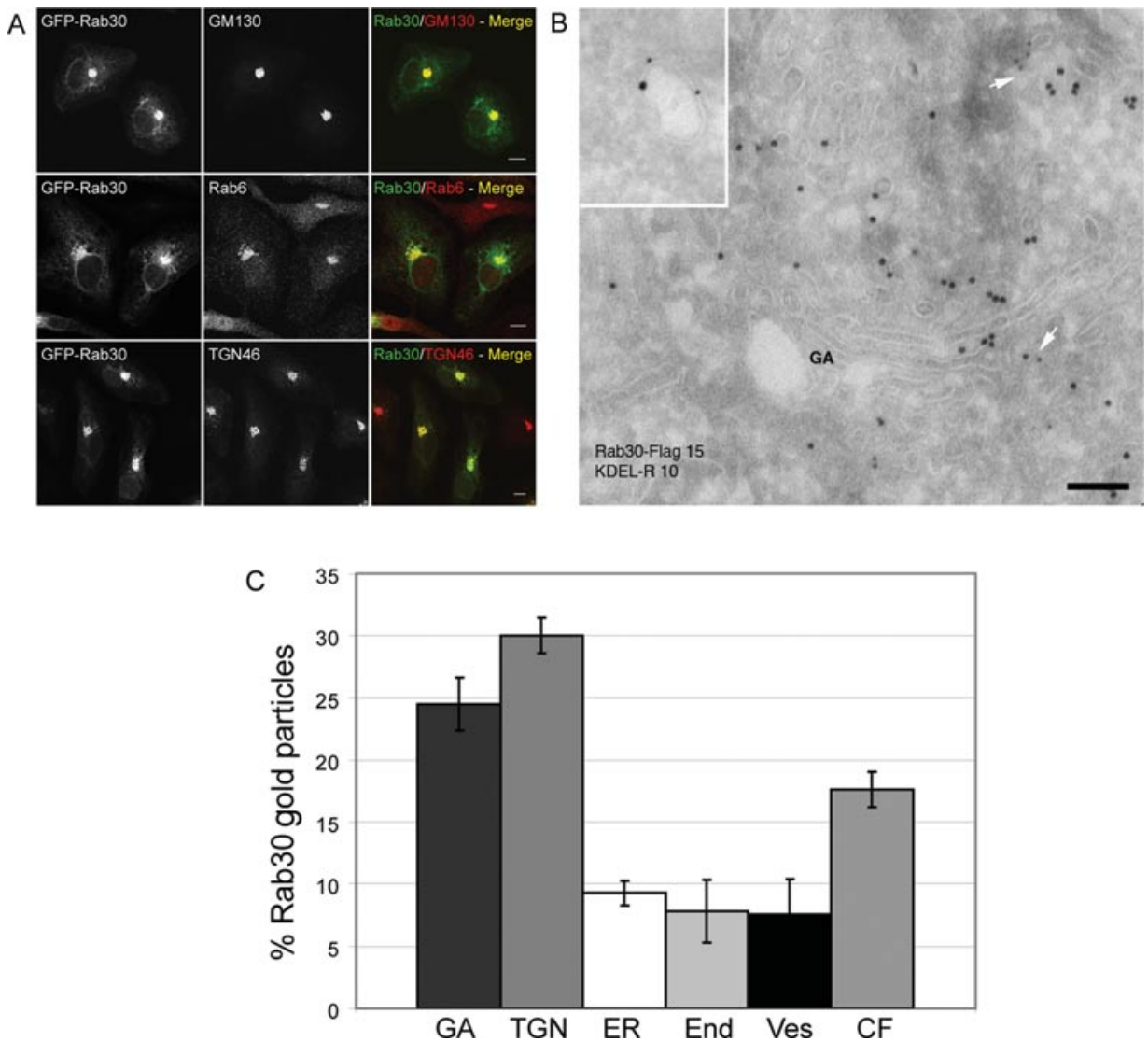

1B and 1C). To further examine the distribution of GFP–Rab30 to Golgi cisternae, HeLa cells transfected with GFP–Rab30 were treated with nocodazole for 3 h to disrupt the microtubule cytoskeleton and fragment of the Golgi apparatus, dispersing the Golgi elements yet maintaining their identity as *cis*-, medial- or *trans*-Golgi and the TGN. Upon nocodazole treatment, GFP–Rab30 continued to display significant co-localisation with *cis*-, medial- and *trans*-Golgi or TGN marker proteins indicating

Figure 2 | GFP–Rab30 associates with *cis*-, medial- and *trans*-Golgi cisternae in nocodazole treated cells
(**A**) HeLa cells were transfected with pEGFP-C1/Rab30. Sixteen to 18 h after transfection, the cells were incubated for 3 h with 10 μM nocodazole. Following this, the cells were processed for immunofluorescence microscopy and immunostained with antibodies to GM130, Rab6 or TGN46. (**B**) Quantification of the proportion of GFP–Rab30-positive structures that are also positive for GM130, Rab6 or TGN46 in nocodazole-treated cells. Figures presented represent the total number of GFP–Rab30 pixels that are also positive for GM130, Rab6 or TGN46 in 16 individual cells in each of three independently performed experiments (mean $\pm$SD). All data are typical of at least three independent experiments. Scale bar indicates 10 μm.

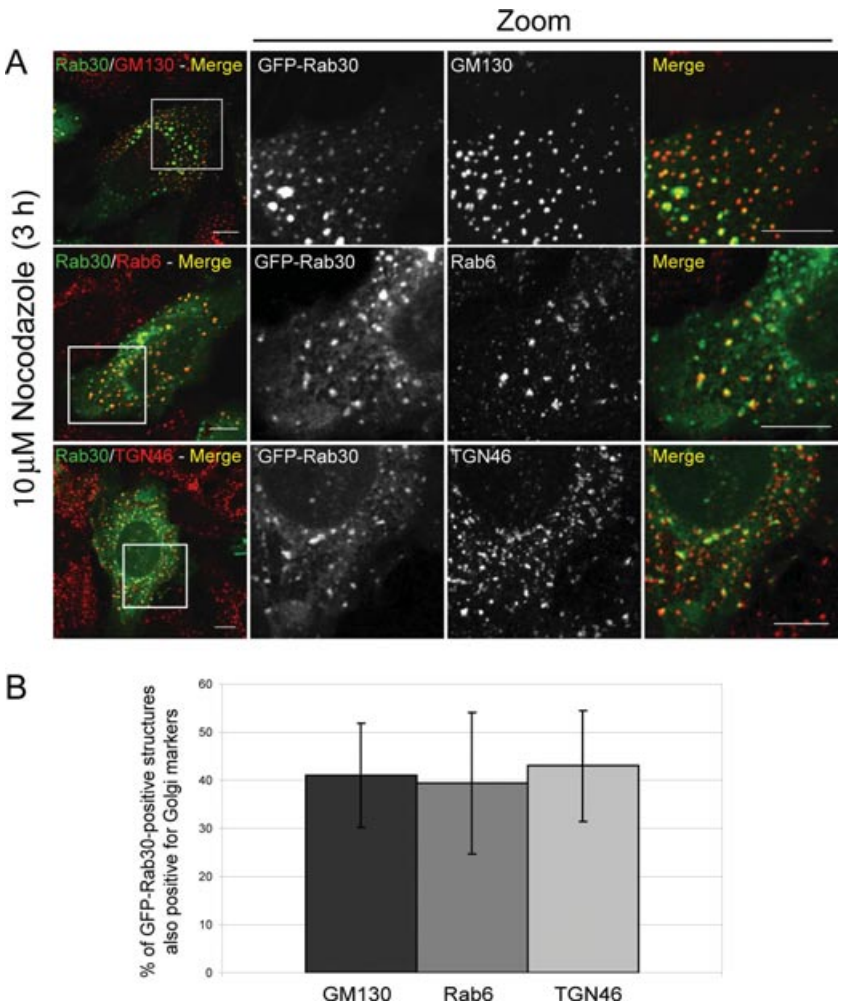

that Rab30 is indeed distributed throughout the Golgi (Figures 2A and 2B). Conversely, little or no co-localisation was evident between GFP–Rab30 and markers of the endocytic pathway including EEA1, LBPA, LAMP1 or Rab11a (Supplementary Figure S1). Notably, minor co-localisation was evident between GFP–Rab30 and the transferrin receptor (TfnR), a marker of the endosomal-recycling pathway (Supplementary Figure S1). However, treatment of cells with nocodazole to allow better distinction to be made between the Golgi and the endosomal-recycling compartment (ERC) revealed that this co-localisation between GFP–Rab30 and the TfnR was markedly reduced. The coincidental co-localisation is most likely due to the proximity of the Golgi and ERC–also known as the recycling endosome–in HeLa cells (data not shown).

To investigate the subcellular distribution of endogenous Rab30, we utilised a commercially available mouse monoclonal anti-Rab30 antibody.

Figure 3 | Endogenous Rab30 and Rab30 Q68L localise to the Golgi and Rab30 T23N localises to the cytoplasm
(**A**) HeLa cells were processed for immunofluorescence microscopy and immunostained with antibodies to Rab30 and Rab6 or TGN46. (**B**) HeLa cells were transfected with pEGFP-C1/Rab30 Q68L. Sixteen to 18 h after transfection, cells were processed for immunofluorescence microscopy and immunostained with antibodies to GM130 or TGN46. (**C**) HeLa cells were transfected with pmCherry-C1/Rab30 T23N. Sixteen to 18 h after transfection, the cells were processed for immunofluorescence microscopy. 4',6-Diamidino-2-phenylindole was used to visualise nuclei. Data are typical of at least three independent experiments. Scale bar indicates 10 μm.

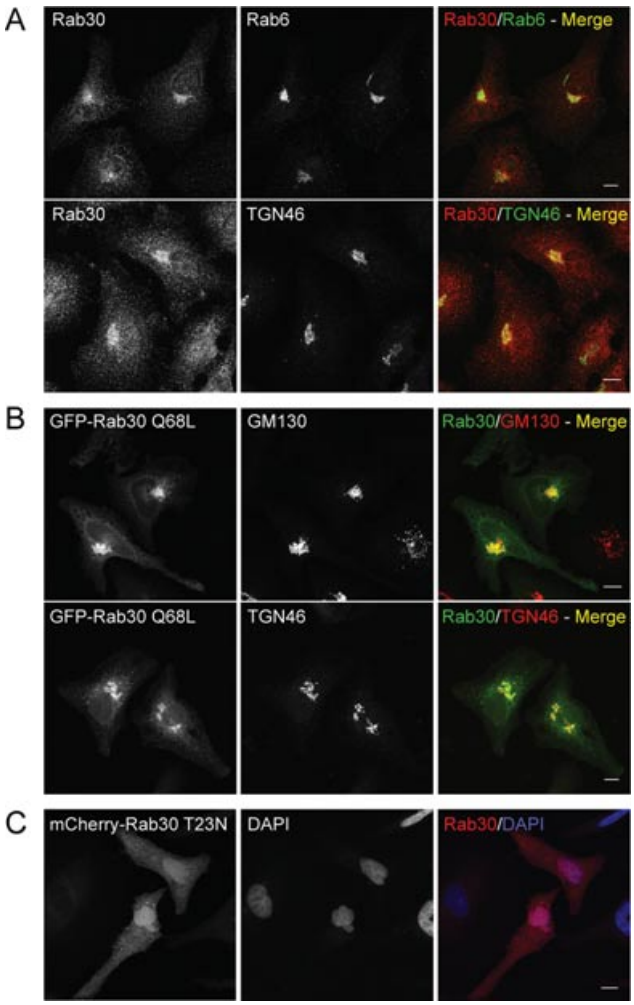

First, we confirmed that this antibody specifically detected Rab30, and not several other Rab GTPases, by immunofluorescence microscopy (Supplementary Figure S2). In agreement with our exogenous GFP–Rab30 data, we found by confocal immunofluorescence microscopy that Rab30 localised to the Golgi where it co-localised with TGN46 and Rab6, whilst also displaying some fine punctate pattern which was dispersed throughout the cell (Figure 3A). To examine the possibility that Rab30 may localise to ER–Golgi intermediate compartments (ERGICs), HeLa cells were incubated at 15°C for 3 h, then fixed and immunolabelled for Rab30 and β-COP, a marker protein of the COPI coat complex. At 15°C, there is impaired delivery of proteins from the ERGIC to the Golgi, resulting in the accumulation of proteins which cycle between the ER and the Golgi on a pre-Golgi 15°C compartment (Saraste and Kuismanen, 1984; Klumperman et al., 1998). We did not observe a shift in Rab30 localisation to peripheral 15°C

Figure 4 | Rab30-positive vesicles are not observed to arrive at or exit the Golgi apparatus
HeLa cells were transfected with pEGFP-C1/Rab30 or pEGFP-C2/Rab6a and time-lapse microscopy performed at 16 h after transfection. The arrows point to a single structure that was monitored over time at 10-s intervals.

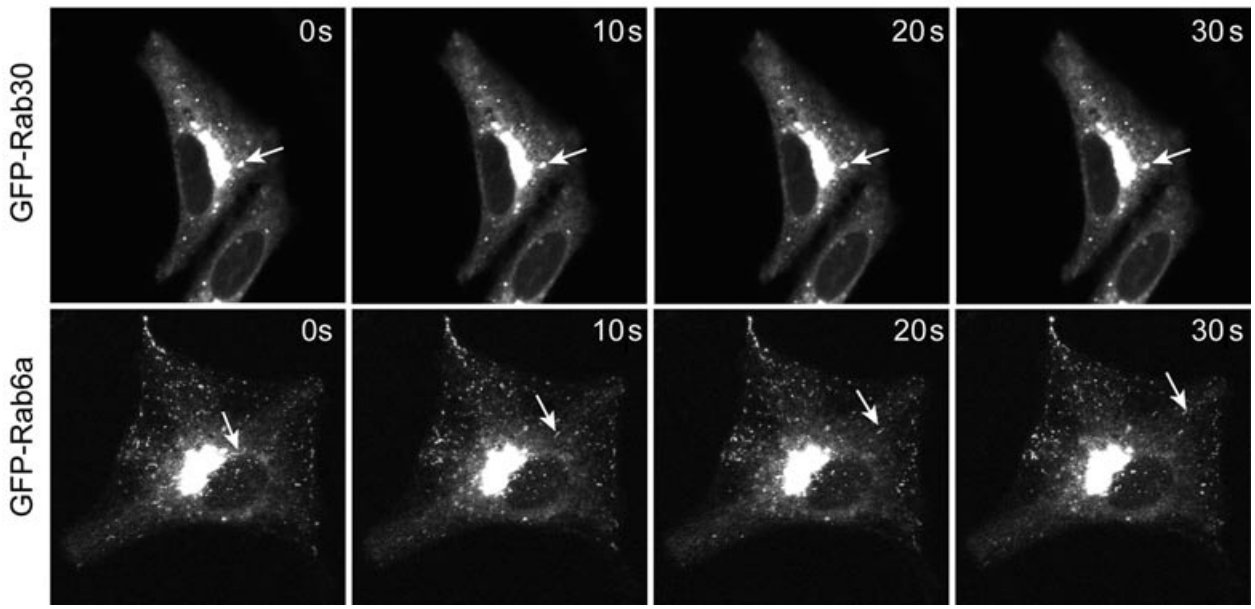

compartments, suggesting that Rab30 does not actively cycle between ERGIC compartments and the Golgi (Supplementary Figure S3). Similar results were observed with exogenous Xpress-fused Rab30 (data not shown).

Several studies have demonstrated that mutations in Rab proteins, equivalent to the Q61L mutation in p21-ras, inhibit both their intrinsic and the GTPase activating protein (GAP)-stimulated GTPase activity, thus locking the mutant in the GTP-bound, and thus 'active', conformation (Tisdale et al., 1992; Stenmark et al., 1994). Confocal immunofluorescence microscopy of this 'active' mutant of Rab30 (Rab30 Q68L) revealed that its distribution broadly mirrored that of the wild-type protein, whereby it co-localised significantly with all Golgi marker proteins tested (Figure 3B), but displayed little or no co-localisation with endosomal proteins (Supplementary Figure S4). We next examined the distribution of the GDP-locked, and thus 'inactive', Rab30 mutant (Rab30 T23N) and found that it was primarily present in the cytosol and nucleus (Figure 3C). In cells expressing relatively high levels of the Rab30 T23N protein, some distribution to punctate structures was also observed (data not shown). To confirm these data, we permeabilised cells prior to fixation to allow the cytosolic fraction to wash out of the cell. After this treatment, we observed that the cytosolic fraction of mCherry–Rab30 T23N was removed in the majority of cells; however, the minority of cells that retained mCherry–Rab30 T23N displayed some punctate pattern in the vicinity of the nucleus and also in dispersed puncta throughout the cell (data not shown). Taken together, these data indicate that Rab30 is primarily associated with the Golgi apparatus.

Rab30 is dynamically associated with the Golgi apparatus

Many Rab GTPases localise to the Golgi apparatus reflecting its role as a central hub of intracellular membrane trafficking in eukaryotic cells. One such Rab, Rab6, localises to the medial- and *trans*-Golgi and functions in retrograde transport through successive Golgi stacks, and to the ER, and has also been implicated in the regulation of exocytic transport from the Golgi (Martinez et al., 1997; White et al., 1999; Sannerud et al., 2003; Grigoriev et al., 2007). To examine the dynamics of Rab30 transport in epithelial cells, we compared GFP–Rab30 to GFP–Rab6a by time-lapse microscopy and fluorescence recovery

after photobleaching (FRAP) experiments. For this work, HeLa cells were plated onto imaging discs, transfected with GFP–Rab30 or GFP–Rab6a and imaged at 10 s intervals for several minutes (Figure 4 and Movies 1 and 2). Time-lapse microscopy revealed that although both Rab30 and Rab6a are primarily associated with the Golgi, no GFP–Rab30-positive vesicles or tubules were observed to enter or exit the Golgi area (Figure 4 and Movies 1 and 2). Indeed, GFP–Rab30-positive material appeared to fluctuate or oscillate in the reticular/cytosolic fraction which is not indicative of long-range vesicular transport to endosomes or the PM (Figure 4 and Movie 1). On the contrary, in HeLa cells, expressing GFP–Rab6a punctate vesicular structures and tubules were readily observed to move from the Golgi area towards the cell periphery, and others were observed to move from peripheral locations towards the Golgi which is characteristic of post-Golgi anterograde and endosomal to Golgi retrograde transport, respectively (Figure 4 and Movie 2).

Next, as Rab30-positive vesicular structures were not observed to enter or exit the Golgi area, we investigated the nature of Rab30 association with the Golgi by selectively photobleaching the Golgi fraction of GFP–Rab30. After photobleaching, we observed considerable recovery (>60% over 6 min) of GFP–Rab30 fluorescence to the Golgi suggesting that Rab30 is continuously and rapidly recruited at the Golgi compartment (Figures 5A and 5B and Movie 3). We compared these results to the same experiment performed with GFP–Rab6a and found that there is comparable recovery to the Golgi area for both these Rab GTPases, both displaying a half-life ($T_{1/2}$) of approximately 10 s (Figures 5A and 5B and Movie 4). To confirm these results, we performed fluorescence loss in photobleaching (FLIP) experiments in which we continuously bleached the Golgi fraction of GFP–Rab30 at 50 s intervals over a period of 594 s (Figure 5C and Movie 5). We found that there is considerable loss of GFP–Rab30 fluorescence from the area excluding the Golgi, again suggesting that there is continuous recruitment of Rab30 onto the Golgi (Figure 5C, upper panel and Movie 5). Equivalent FLIP experiments on the non-Golgi region revealed that there is some local loss of cellular fluorescence in proximity to the site of bleaching, and some loss from bulk of the GFP–Rab30 labelling at the Golgi; however, the majority of the cellular fluorescence remains within the cell (Figure 5C, lower panel and Movie 6).

To further explore the trafficking dynamics of Rab30, we performed a FRAP experiment whereby the non-Golgi fractions of GFP–Rab30 and GFP–Rab6a were photobleached. We found that the recovery GFP–Rab30 to the non-Golgi region was exclusively cytosolic with no distinct vesicular structures or tubules observed to exit the Golgi area (Figure 5D and Movie 7). These data are in agreement with our previous FLIP experiment of the non-Golgi region suggesting that the non-Golgi fraction of GFP–Rab30 is principally cytosolic and not indicative of directional vesicular trafficking. In contrast, GFP–Rab6a displayed distinct, numerous and rapidly moving vesicles exiting the Golgi area 10 s after photobleaching and continuing for the duration of recording (Figure 5D and Movie 8).

We also examined the dynamics of GFP–Rab30 in nocodazole-treated cells. In the absence of microtubules, there is little or no movement of GFP–Rab30-positive material with the exception of random fluctuations of the cytosolic fraction (Movie 9). Interestingly, dispersed GFP–Rab30 fragments due to nocodazole treatment showed significant recovery during FRAP experiments, suggesting that GFP–Rab30 is recruited onto Golgi membranes independent of the integrity of the microtubule cytoskeleton (Movie 10).

Taken together, these data suggest that although Rab30 and Rab6a are both distributed to the Golgi, and associate dynamically with this compartment, they likely serve distinct cellular roles on this organelle and that Rab30 is primarily recruited to the Golgi from the cytosol.

Depletion of Rab30 disrupts the structural integrity of the Golgi

The data outlined above suggest a role for Rab30 in the regulation of intracellular trafficking along the secretory pathway. To investigate the functional effects of depletion of Rab30, HeLa cells were transfected with control or one of two Rab30-specific small interfering RNA (siRNA) oligonucleotides, and efficient knockdown of Rab30 was confirmed by reverse-transcription polymerase chain reaction (RT-PCR) and Western blotting (Figures 6A and 6B).

Electron microscopy (EM) analysis of control siRNA-treated cells revealed a typical Golgi

Figure 5 | Rab30 associates dynamically with the Golgi apparatus

(**A**) HeLa cells were transfected with pEGFP-C1/Rab30 or pEGFP-C2/Rab6a and time-lapse microscopy performed 16 h after transfection. The Golgi area (indicated by ROI outline) was bleached on 100% laser power for 125 iterations. Recovery to the ROI was recorded at 10 s intervals for 350 s. (**B**) Quantification of fluorescence recovery to the ROI is the mean of five recordings each for three independently performed experiments (mean ±SD). (**C**) HeLa cells were transfected with pEGFP-C1/Rab30 and time-lapse microscopy performed at 16 h after transfection. The ROI was bleached on 100% laser power for 125 iterations at 50 s intervals for the indicated time. Images were recorded at 10 s intervals. (**D**) HeLa cells were transfected with pEGFP-C1/Rab30 or pEGFP-C2/Rab6a and time-lapse microscopy performed at 16 h after transfection. Non-Golgi area (indicated by two distinct ROI outlines) was bleached on 100% laser power for 125 iterations. Recovery to the ROI was recorded at 10 s intervals for a total of 280 s. The arrows point to vesicles that emanated from the Golgi area after bleaching. All data are typical of at least three independent experiments. Scale bar indicates 10 μm.

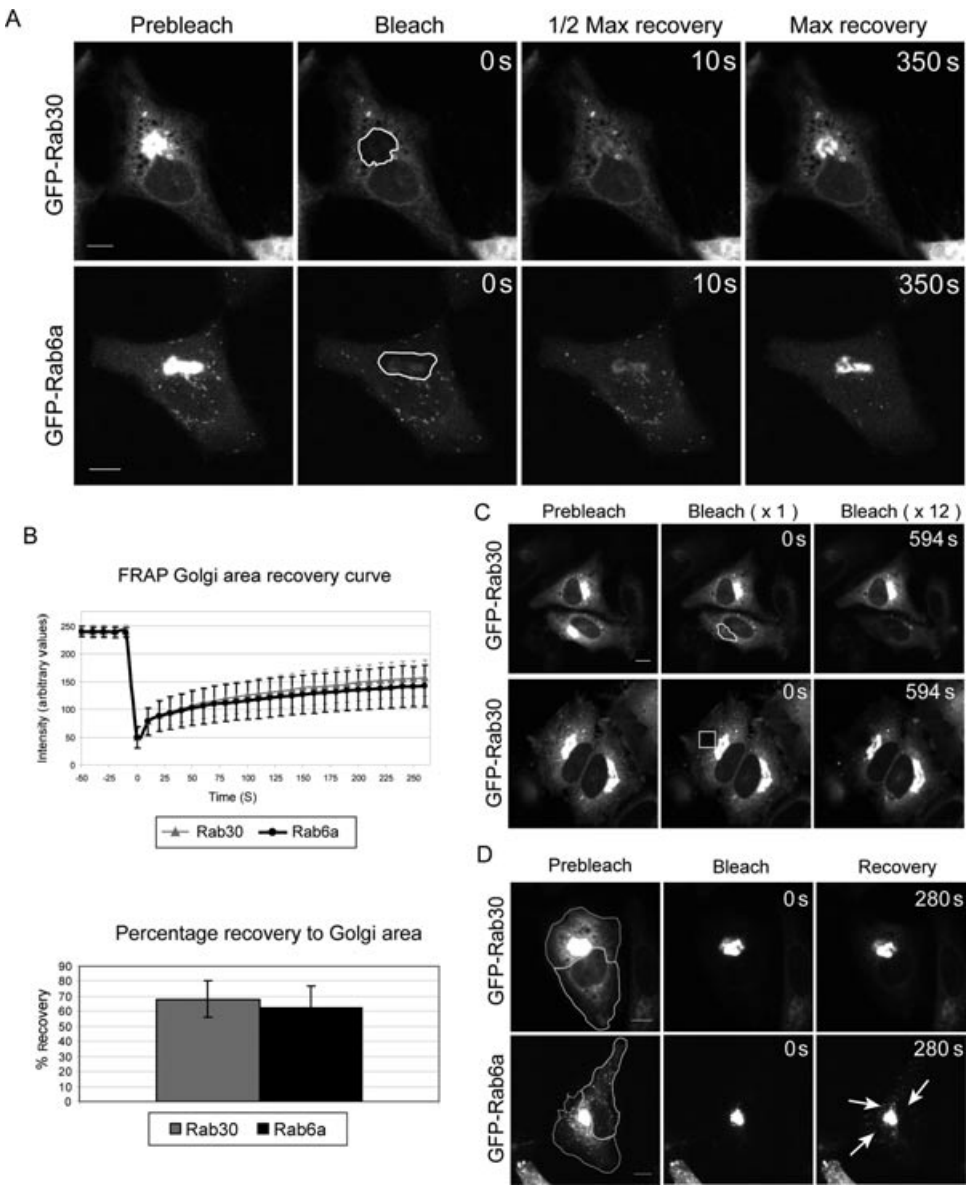

Figure 6 | Rab30 is essential for normal Golgi morphology

(**A**) Quantitative RT-PCR of siControl (siCtrl)- or Rab30 siRNA (siRAB30)-treated HeLa cells. *y*-axis: $2^{\wedge}(-dCt)$ value represents differences between the mean Ct (cycle threshold) values of Rab30 gene and reference gene (S26). (**B**) Western blot analysis of lysates from cells treated with control or RAB30 siRNAs using anti-Rab30 and anti β-tubulin as a loading control. (**C–F**) HeLa cells treated with control (siCtrl; **C** and **D**) or Rab30 (siRAB30; **E** and **F**) siRNAs were analysed by conventional EM. (**D**) and (**F**) are higher magnifications of Golgi area in (**C**) and (**E**), respectively. GA, Golgi apparatus; End, endosome; Lys, lysosome; N, nucleus; m, mitochondria. Scale bar indicates 0.8 μm. (**G**) Quantification of the number of Golgi structures in Rab30-depleted and control cells. Data are presented as percentage (mean $\pm$SD). (**H**) Measure of the length (nm) of Golgi cisternae in Rab30-depleted and Ctrl cells. Values (nm) are the mean of two separate experiments $\pm$SD.

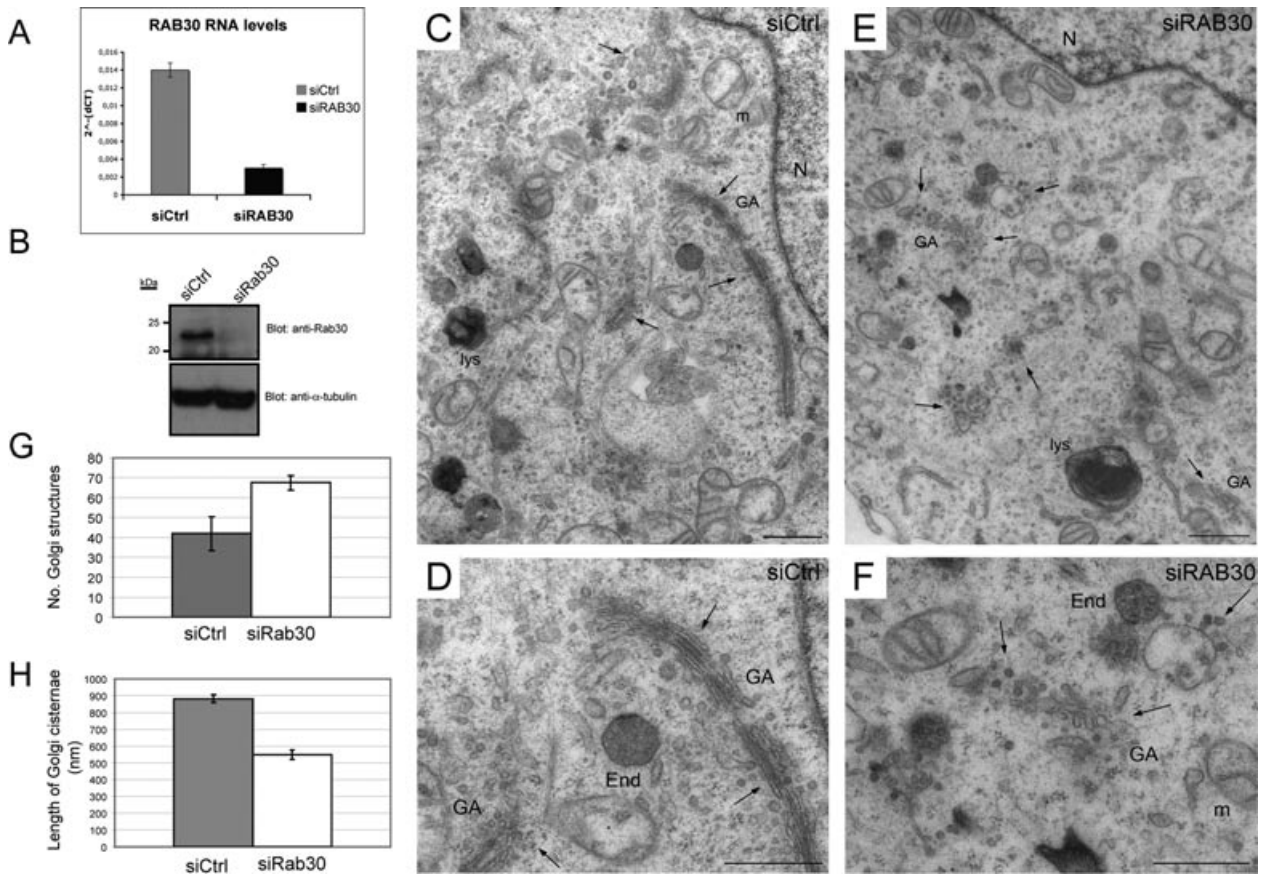

morphology in which the normal cisternal structure of the Golgi stacks is positioned in the juxtanuclear region of the cell (Figures 6C and 6D). Interestingly, we found in cells depleted of Rab30 that the morphology of the Golgi apparatus was significantly perturbed, such that the normal Golgi cisternae were mostly abnormal and fragmented (Figures 6E and 6F). We found that siRab30 cells displayed significantly more Golgi fragments than in siCtrl-treated cells and conversely, the length of Golgi cisternae in the control cells was notably longer than those in siRab30 cells (Figures 6G and 6H).

To further investigate the phenotypic effect of Rab30 knockdown, we performed confocal immunofluorescence microscopy in which HeLa cells were transfected with independent control and Rab30-targeting siRNA oligonucleotides and immunostained with a range of Golgi marker proteins (Figures 7A and 7B). In agreement with our EM data (Figure 6), and using a distinct Rab30 siRNA, we observed that GM130, Rab6 and TGN46 localisation was altered from the compact Golgi structure observed in control cells, to a scattered, and in some cases tubulated, morphology in Rab30-depleted cells

Figure 7 | Rab30 is required for normal Golgi morphology

(**A**) HeLa cells were transfected with control or Rab30 siRNA. Seventy-two h after transfection, cell lysates were analysed by Western blot with the anti-Rab30 antibody and anti-β-actin as a loading control. (**B**) HeLa cells were treated with control- or Rab30-specific siRNA. At 72 h after transfection, cells were processed for immunofluorescence microscopy and immunostained with antibodies to GM130, Rab6 or TGN46. (**C**) Quantification of Golgi fragmentation because of Rab30 knockdown. Fifteen fields of cells, for each of three independently performed experiments, containing an average of 34 and minimum of 16 cells were counted and the degree of Golgi fragmentation scored on the basis of dispersed or compact GM130 distribution. Figures represent the mean $\pm$SD. (**D**) HeLa cells were treated with Rab30 siRNA. Fifty-four h after transfection, cells were transfected with siRNA resistant pEGFP-C1/Rab30. Sixteen h later, the cells were processed for immunofluorescence microscopy and immunostained with an antibody to TGN46. (**E**) HeLa cells were transfected with pmCherry–Rab30 T23N. Sixteen h after transfection, cells were processed for immunofluorescence microscopy and immunostained with an antibody to TGN46. All data are typical of at least three independent experiments. Scale bar indicates 10 μm.

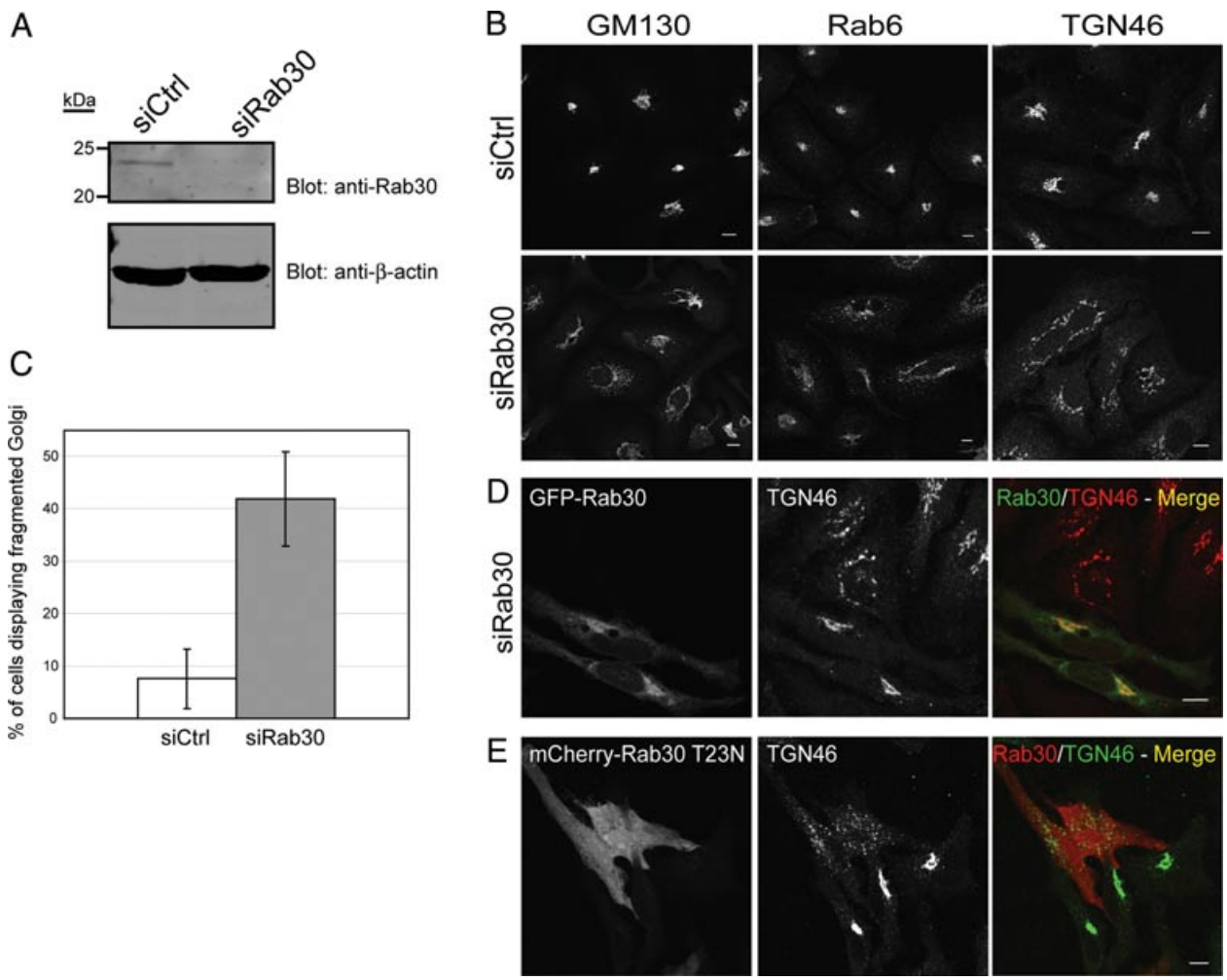

(Figure 7B). Quantification of this data revealed that approximately 41% of siRab30-treated cells displayed an abnormal Golgi apparatus compared with approximately 8% for control (Figure 7C). Interestingly, markers of other cellular compartments, including endosomes and lysosomes, remained largely unaffected in Rab30-depleted cells (data not shown). We confirmed that the effect of Rab30 knockdown on Golgi morphology was specific by demonstrating that the phenotype could be reversed through the

introduction of GFP–Rab30 which is not targeted by the Rab30 siRNA (Figure 7D). In further support of these data, we found that HeLa cells transfected with the mCherry-fused dominant-negative Rab30 mutant (Rab30 T23N) also displayed a fragmented and scattered Golgi apparatus (Figure 7E). Taken together, these data indicate that Rab30 is essential for the perinuclear distribution and structural integrity of the Golgi apparatus.

Perturbation of Rab30 function does not affect the trafficking of anterograde or retrograde cargo through the secretory pathway

To investigate the role of Rab30 in intracellular transport events within the Golgi, we performed a number of trafficking assays to assess the involvement of Rab30 in anterograde and retrograde transport events through this organelle. To determine the ability of Rab30 to influence the trafficking of material through the secretory pathway, we utilised the vesicular stomatitis virus glycoprotein (VSV-G) tsO45 protein trafficking assay. VSV-G tsO45 is a temperature-sensitive mutant of VSV-G which traffics from the ER to the Golgi and subsequently onwards to the PM (Presley et al., 1997). At the non-permissive temperature of 40°C, this mutant remains 'blocked' in the ER; however, this block can be released by shifting the cells to the permissive temperature of 32°C, sending a wave of VSV-G tsO45 from the ER to the Golgi when *de novo* protein biosynthesis is halted by treating cells with cycloheximide (Presley et al., 1997) (Figure 8A). To investigate the functional effects of Rab30 on the trafficking of VSV-G tsO45, we co-expressed YFP/VSV-G tsO45 with mCherry–Rab30 or mCherry–Rab30 T23N and performed the trafficking assay as outlined above. Upon shifting cells expressing to the permissive temperature, we found that VSV-G moved from the ER to the Golgi after 20 min and was observed at the PM and peripheral cytoplasmic vesicles after 120 min, indicating that the overexpression of Rab30 or Rab30 T23N does not affect the trafficking of VSV-G through the secretory pathway (Figure 8A, Supplementary Figure S5 and data not shown).

We next examined the effect of Rab30 depletion on the localisation of β1, 4-galactosyltransferase I (GalT), an enzyme which cycles slowly between the ER and the Golgi and thus acts as an endogenous indicator of transport between these compartments (Nilsson et al., 1991; Storrie et al., 1998). We found that in control or Rab30 siRNA-treated cells, GalT was capable of accessing the Golgi apparatus as evinced by co-localisation between GalT and TGN46 (Figure 8B). To further examine anterograde transport processes, we performed an experiment utilising brefeldin A (BFA), a fungal metabolite that acts as an interfacial inhibitor of ARF GTPase activation resulting in the tubulation of Golgi membrane and the redistribution of Golgi membrane into the ER (Klausner et al., 1992; Mardones et al., 2006). Retrograde Golgi-to-ER transport was induced by initially treating cells with BFA (for example, see Figure 9B) followed by washout to allow ER–Golgi transport to proceed normally. We found that upon BFA washout, both GalT and GM130 were transported to a fragmented, albeit reforming, Golgi apparatus after 1 h in both control siRNA and siRab30-treated cells (Supplementary Figure S6). These data further suggest that Rab30 does not play a role in anterograde ER-to-Golgi trafficking processes.

To investigate the role of Rab30 in retrograde transport we followed the trafficking of cholera toxin fragment B (CTxB) in Rab30-depleted HeLa cells. CTxB binds to the GM1 cell surface receptors and is transported to the ER via endosomes and the Golgi (Lencer and Tsai, 2003). For this work, HeLa cells were treated with control or Rab30-specific siRNA and allowed to internalise Alexa Fluor-594 labelled CTxB. In both control and siRab30-treated cells, CTxB reached the Golgi compartment after 30 min of uptake, followed by a 1 h chase (Figure 9A, upper panels). These data suggest that Rab30 does not function in the transport of material from the cell surface to the Golgi. Similarly, after a 6 h chase, CTxB was transported through the Golgi compartment and onwards to the ER (Figure 9A, lower panels). Following a 6 h chase, we found that the distribution of CTxB was unaffected by depletion of Rab30 (Figure 9A, lower panels). These data indicate that Rab30 does not function in the transport of CTxB from the Golgi to the ER. We also examined the distribution of a GM130 and GalT upon BFA treatment in the context of Rab30 depletion. We observed that GM130 and GalT were similarly distributed to ER exit sites and the ER, respectively, in both control and siRab30-treated cells indicating that BFA-induced retrograde Golgi-to-ER transport was unaffected by depletion of Rab30 (Figure 9B).

Figure 8 | Rab30 does not affect anterograde transport of VSV-G tsO45 or GalT

(**A**) HeLa cells were transfected with the indicated plasmid constructs and incubated at 37°C or 8–10 h. Cells were then moved to 40°C for a further 12 h in order to accumulate VSV-G on the ER (time 0). Cells were washed and fixed in 3% PFA or washed and the media replaced with complete DMEM supplemented with 50 μg/ml cycloheximide and transferred to a 32°C incubator for a further 20 or 120 min. Cells were then processed for immunofluorescence microscopy. (**B**) HeLa cells were treated with control- or Rab30-specific siRNA. At 72 h after transfection, cells were processed for immunofluorescence microscopy and immunostained with antibodies against TGN46 and GalT. All data are typical of at least three independent experiments. Scale bar indicates 10 μm.

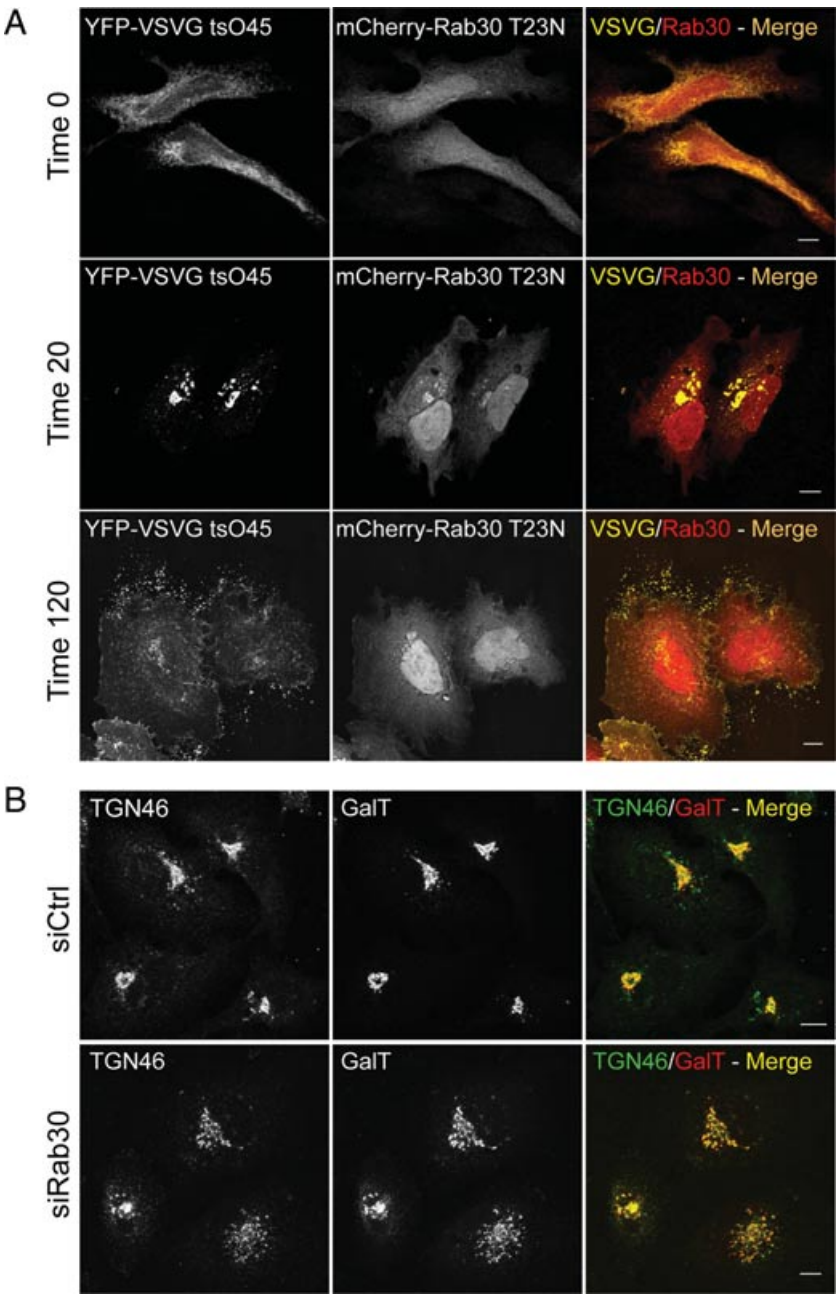

Figure 9 | Rab30 does not affect retrograde trafficking of cholera toxin to the Golgi or ER

(**A**) HeLa cells treated with siCtrl or siRab30 were allowed to continuously internalise AlexaFluor-594 labelled CTxB for 30 min. Following this, cells were washed extensively with PBS before incubation with normal DMEM for the indicated time points, fixed, processed for immunofluorescence microscopy and immunostained with an antibody to TGN46. (**B**) HeLa cells treated with siCtrl or siRab30 were treated with 5 μg/ml of BFA for 30 min, processed for immunofluorescence microscopy and immunostained with an antibody to GM130 or GalT. All data are typical of at least three independent experiments. Scale bar indicates 10 μm.

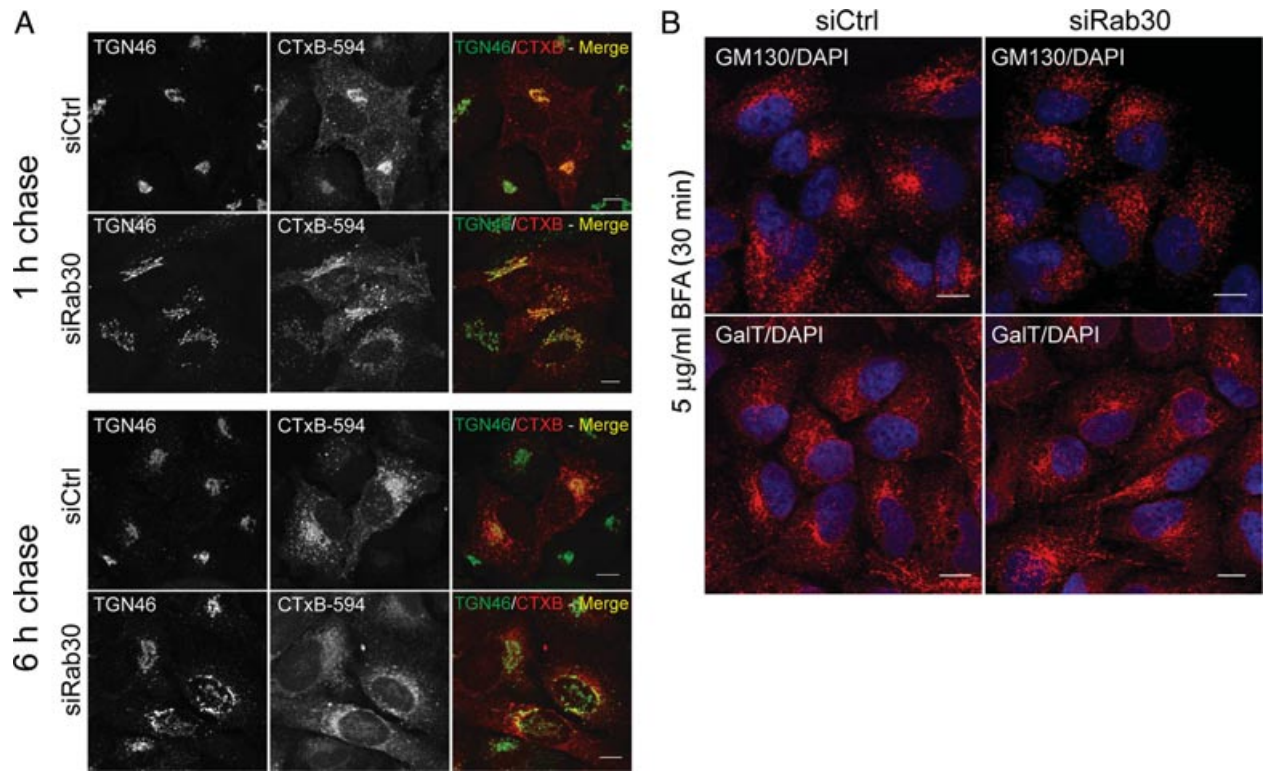

Taken together, these data suggest that Rab30 is unlikely to play a critical role in the anterograde transport pathway from the ER to the PM via the Golgi apparatus or in the retrograde transport pathway from the PM to the ER.

Discussion

The critical role served by the Rab family of small GTPases in all aspects of intracellular membrane trafficking has led to their intensive study and characterisation over the past 20 years. Many Rabs have been studied at length, whereas others have received relatively little attention. Rab30 has previously been shown to associate with the Golgi compartment in several non-human cell lines but its functional role has remained largely elusive (de Leeuw et al., 1998; Sinka et al., 2008; Thomas et al., 2009).

Several membrane trafficking processes occur along the secretory pathway through the Golgi apparatus. In the anterograde pathway, material leaves the ER at ER-exit sites where it is packaged into COPII coated vesicles which fuse with each other to form ERGICs (Lee et al., 2004). These ERGICs then fuse together to form new *cis*-Golgi cisternae as the existing Golgi cisternae matures to medial-Golgi, *trans*-Golgi and TGN with subsequent accumulation and packaging at the TGN for onward trafficking to the PM for excretion or to other intracellular destinations (Lee et al., 2004). Conversely, the retrograde transport pathway material arrives at the Golgi at the TGN where it is transported through successive Golgi stacks to the ERGIC and the ER. Efficient secretory pathway transport requires complex interplay between several protein families, including small GTPases, coat proteins, microtubule-based

motors, golgins and tethering proteins (Lee et al., 2004; Short et al., 2005). In order to gain insight into the possible role of Rab30 in secretory pathway trafficking processes, we performed a detailed subcellular distribution analysis and number of time-lapse microscopy experiments using GFP-fused Rab30. We have demonstrated here that Rab30 is principally associated with the Golgi compartment where it is distributed to each of the Golgi cisternae. Our analysis of GFP–Rab30 by time-lapse microscopy and its intracellular localisation and analysis of trafficking assays implies that Rab30 is not primarily involved in trafficking at pre- or post-Golgi compartments, suggesting its function lies within the Golgi apparatus.

We have observed here that depletion of Rab30 results in a dramatic alteration of the morphology of the Golgi apparatus. A number of Rab30-mediated cellular mechanisms could explain this phenotypic effect. The cisternal maturation model for ER-to-Golgi and subsequent intra-Golgi transport predicts that the formation of new Golgi cisternae occurs from the fusion of ERGIC that mature to form the *cis*-face of the Golgi which itself subsequently matures to form the medial- and *trans*-Golgi cisternae (Glick and Malhotra, 1998; Pelham, 1998). As such, a blockade of secretory cargo can prevent the fusion of new membrane from ERGICs at the *cis*-Golgi, thus disrupting the formation of new cisternae and leading to a scattering effect of the Golgi compartment. However, we have observed that depletion/inactivation of Rab30 does not influence the ability of anterograde cargoes to move through the secretory pathway, indicating that loss of the loss Golgi integrity is not likely because of a blockade in anterograde transport.

Despite the dramatic effect of Rab30 knockdown on the morphological integrity of the Golgi apparatus, neither anterograde nor retrograde transport appears to be perturbed. However, it is known that the Golgi is capable of maintaining its function when its integrity is severely disrupted, as in the case of drug disruption of microtubules (Rogalski et al., 1984). As such, depletion of Rab30 could disrupt Golgi structural integrity without grossly affecting fundamental Golgi trafficking processes. Indeed, although several cases have been documented in *D. melanogaster* where there is a lack of correlation between loss of Golgi architecture and transport efficiency, such cases in mammalian cells are rare (Kondylis and Rabouille, 2009). Despite this, depletion of a number or proteins such as Golgin-84, a Rab1 effector, is known to result in the loss of Golgi organisation without inhibiting anterograde transport processes (Diao et al., 2003). Recent reports have indicated that Rab30 is capable of interacting with the *D. melanogaster* orthologues of several members of a family of extensive coiled-coil proteins known as golgins (Sinka et al., 2008). These golgins are recruited in a tightly regulated manner to the cytoplasmic face of Golgi membranes where they are believed to function as scaffold molecules to bind an array of protein partners (Goud and Gleeson, 2010). Rab GTPases are now believed to be important players in the regulation of golgin function. Several reports have demonstrated that Rab GTPases are known to directly recruit golgins to specific membrane subdomains. These include the direct recruitment of BicD by Rab6 and of p115 by Rab1 (Allan et al., 2000; Matanis et al., 2002; Short et al., 2002). Rab30 has been shown to bind the *D. melanogaster* orthologues of several human golgins including, BicD, p115, Golgin-97, GCC88, Golgin-245 and GM130 (Sinka et al., 2008). Although it has not been confirmed that Rab30 directly binds these golgins in mammalian cells, it is tempting to speculate that loss of recruitment by Rab30 of one or many of these golgins to Golgi cisternae could result in the overall loss of Golgi structural integrity. The characteristics of Golgi remnants after knockdown can vary substantially depending on the degree of fragmentation of particular cells; however, for the most part, it appears that they are indicative of a loss of cohesion between Golgi membranes which may be because of the unlinking of distinct Golgi cisternae. Indeed, similar effects on the morphology of the Golgi have also been observed upon disruption of the function of golgins such as p115 and GM130 (Alvarez et al., 1999; Puthenveedu and Linstedt, 2001; Puthenveedu et al., 2006). Clearly, further investigation of the interactions between Rab30 and its putative effector golgins will be required to determine if this is the cause of loss of Golgi integrity during Rab30 depletion/inactivation.

It may also be the case that Rab30 does not directly recruit golgins to Golgi cisternae but may regulate and organise the function of golgins already localised to Golgi membranes. Indeed, GM130 is known to interact with Rab1, Rab2 and Rab33b; however, it is known to be dependent on GRASP65 for membrane

association (Barr et al., 1998). Rab30 may regulate golgin insertion or extraction from particular Golgi membranes or facilitate conformational changes in golgin structure, thus modulating the function of the golgin in the membrane. It is possible that the primary function of Rab30 is to regulate and organise the function of golgins and thus, loss of Rab30 function could result in the unlinking and separation of Golgi membranes. Indeed, inactivation of other Golgi-associated Rabs known to associate with golgins such as Rab1 and Rab2 are known to result in loss of Golgi structural integrity (Wilson et al., 1994; Haas et al., 2007). Given that Rab30 appears to interact with a broad subset of golgins (both TGN and *cis*-Golgi), it is possible that Rab30 performs a generalised function in regulating golgin dynamics and may perform synergistic function with other Rab GTPases such as Rab1, Rab2 or Rab6 in performing essential membrane trafficking events linked to Golgi organisation.

Previous work has suggested that Rab30 co-localises with TGN46 and Rab11a on the TGN and may regulate exocytic trafficking from the Golgi compartment to the PM in *D. melanogaster* S2 cells (Thomas et al., 2009). Although we did observe co-localisation between Rab30 and TGN46, our time-lapse microscopy analyses of Rab30 demonstrate that GFP–Rab30-positive vesicles or tubules do not exit the Golgi compartment, nor do they enter the Golgi area from peripheral endosomal structures. Indeed, our data support the recruitment of Rab30 from the cytosol as recruitment is still observed in the absence of the integrity of the microtubule cytoskeleton. It is also interesting to note that FRAP of other Golgi Rab GTPase have been known to show full recovery to the Golgi, such as that of Rab1b, but with a slower $T_{1/2}$ than that observed for Rab30 (Monetta et al., 2007). This may be indicative of direct recruitment of Rab30 to the Golgi from the cytosol rather than its arrival from subcellular compartments such as the ERGIC. Furthermore, we have observed that depletion of Rab30 does not affect the ability of CTxB to access the Golgi or the ER in the retrograde transport pathway. Given the subcellular distribution, trafficking dynamics, inactivation phenotype and previously published interactions with Golgi matrix proteins, the model that we favour for Rab30 function is in the maintenance of Golgi structural integrity via interactions with golgin proteins. Despite this, a role for Rab30 in intra-Golgi transport or in cargo selection cannot be ruled out.

In summary, we have characterised the distribution of Rab30 in HeLa cells, shown that it dynamically associates with the Golgi apparatus and demonstrated that it is necessary to maintain the structural integrity of this organelle. The challenge now remains to identify and characterise the machinery regulating Rab30 function in order to further understand the functional significance of this small GTPase.

Materials and methods

Plasmid constructs

pEGFP-C1/Rab30 and pmCherry-C1/Rab30 were constructed using a forward primer (5′-AAAGGATCCATGAGTATGGAAGATTATGATTTC-3′) and a reverse primer (5′-AAAGGATCCTTAGTTGAAATTACAACAAGTCAA-3′) to amplify human Rab30 cDNA from pGEX-2T Rab30 (kindly provided by Dr Bruno Goud). The 612bp PCR fragment was subsequently cloned into the *Bam*HI site of pEGFP-C1 or pmCherry-C1 (Clontech). pFLAG–Rab30 was constructed using a forward primer (5′-CCCAAGCTTAGTATGGAAGATTATGATTTCCT-3′) and a reverse primer (5′-CGCGGATCCTTAGTTGAAATTACAACAAGTCAA-3′) to amplify human Rab30 coding sequence from cDNA extracted from HeLa cells. The 612bp PCR fragment was subsequently cloned into *Hind*III/*Bam*HI-digested site of p3XflagCMV10 (Sigma). pEGFP-C1/Rab30 Q68L was created by site-directed mutagenesis (SDM) on the corresponding wild-type plasmids using a forward primer (5′-GGGACACAGCAGGTCTAGAGAGATTTCGGTC-3′) and a reverse primer (5′-GACCGAAATCTCTCTAGACCTGCTGTGTCCC-3′). pmCherry-C1/Rab30 T23N was created by SDM on the corresponding wild-type plasmid using a forward primer (5′-GCAACGCTGGTGTGGGGAAGAATTGCCTCGTCCG-3′) and a reverse primer (5′-CGGACGAGGCAATTCTTCCCCACACCAGCGTTGC-3′). pEGFP-C2/Rab8a was constructed using a forward primer (5′-AAAAGAATTCGCGAAGACCTACGATTAC-3′) and a reverse primer 5′-AAAAGTCGACGTCGACAAGGCGGTGTTCCTCACA-3′) to amplify human Rab8a cDNA. The resulting 634bp PCR fragment was cloned into the EcoRI/SalI-digested site of pEGFP-C2 (Clontech). pEGFP-C2 Rab6a was generated by subcloning the EcoRI 624bp fragment from the previously described pLexA/Rab6a construct (Janoueix-Lerosey et al., 1995). pEGFP-C3/Rab11a has been previously described (Kelly et al., 2010). pYFP/VSV-G tsO45 was previously described and a kind gift from Dr Jeremy Simpson (Presley et al., 1997). All constructs made by PCR were verified by DNA sequencing.

Antibodies and Western blotting

Primary antibodies used were mouse monoclonal anti-TfnR (Zymed), EEA1 (BD Transduction Laboratories), GM130 (BD Transduction Laboratories), LBPA (kind gift from Jean Gruenberg), LAMP1 (Abcam), β-actin (Sigma) and Rab30 (Abcam: ab76622); rabbit polyclonal anti-human Rab11a (Zymed), Rab6 (Santa Cruz) (Abcam) β-COP (kind gift from Jeremy Simpson) and sheep polyclonal anti-TGN46 (Serotec). Anti-flag

(Sigma) and anti-human KDEL-R (kind gift from H. Pelham) were used for IEM. Secondary antibodies used were goat anti-mouse conjugated to Alexa Fluor-488 or Alexa Fluor-594, goat anti-sheep conjugated to Alexa Fluor-488 or Alexa Fluor-594, goat anti-rabbit Alexa Fluor 488 (all Molecular Probes) and donkey anti-rabbit conjugated to indocarbocyanine (CY3) (Jackson ImmunoResearch). Protein A–gold (PAG) was purchased from Cell Microscopy Centre, Utrecht, the Netherlands. Nuclei were visualised using 4′,6-diamidino-2-phenylindole (Sigma). Western blotting was performed as previously described (Giordano et al., 2009; Kelly et al., 2010). For Western blotting, the secondary antibody used were anti-mouse horseradish peroxidase conjugated (Jackson ImmunoResearch) or anti-mouse and IRDye680 (LI-COR).

Cell lines, plasmid transfection and RNAi

The HeLa (human cervical carcinoma) cell line was cultured in Dulbecco's modified Eagle medium (DMEM) supplemented with 10% v/v foetal bovine serum, 2 mM L-glutamine and 25 mM 4-(2-hydroxyethyl)-1-piperazineethanesulfonic acid (HEPES) and grown in 5% CO_2 at 37°C. For overexpression studies, cells were transfected with plasmid constructs using Lipofectamine 2000 (Invitrogen) as transfection reagent. Rab30 expression in HeLa cells was depleted by transfection with a duplex of the following siRNA oligonucleotides Rab30 (5′-AAGAGAGATTTCGGTCCATTA-3′) (QIAGEN) which targets the coding sequence of Rab30 and was used for EM experiments; and (5′-GCATTAGCAGAACATATAA-3′) (Sigma) which targets the 3′ UTR of Rab 30 and was used for immunofluorescence experiments. As a control, cells were transfected with small interfering non-targeting oligonucleotides (Sigma and QIAGEN). Control or Rab30 siRNA was transfected using Lipofectamine 2000 according to the manufacturer's instructions (Invitrogen). All siRNA knockdown experiments were carried out over a period of 72 h.

Quantitative real-time PCR

Total RNA was extracted from siRAB30 and control transfected HeLa cells using RNeasy Mini Kit (Qiagen) according to the manufacturer's instructions. Equal amounts of cDNA were synthesised using Superscript II (Invitrogen) and random primers. Real-time PCR was carried out with the ABI PRISM 7000 HT Sequence Detection System (Applied Biosystems) as previously described (Giordano et al., 2007). The following primers were used for quantitative PCR: Rab30 forward (5′-CTGTGAGGAATCCTTCCGTT-3′) and reverse (5′-AACC TCTCTCCTTTCAGCCA-3′), and control S26 forward (5′-CCGTGCCTCCAAGATGACAA-3′) and reverse (5′-GCAA TGACGAATTTCTTAATGGCC-3′).

Immunofluorescence microscopy

Immunofluorescence microscopy was performed as described previously (Horgan et al., 2005). For BFA treatments, cells were washed once with phosphate-buffered saline (PBS) and incubated for 30 min with 10 μg/ml of BFA diluted in complete DMEM before being processed for immunofluorescence microscopy. For BFA washout experiments, cells were washed once with PBS and incubated for 30 min with 10 μg/ml of BFA diluted in complete DMEM, cells were then washed three times with PBS before being incubated for 60 min with fresh complete DMEM. For 15°C incubations, cells were removed from the 37°C incubator washed twice in PBS and overlaid with complete DMEM cooled to 15°C. Cells were then incubated for 3 h in a 15°C water bath before being processed for immunofluorescence microscopy. For nocodazole treatments, cells were overlaid with complete DMEM supplemented with 10 μM of nocodazole for 3 h at 37°C. Co-localisation quantification analyses were performed using the co-localisation module of the Zeiss ZEN software. All fluorescent micrographs shown are three-dimensional projections from the optical sections of the entire Z-stack. For quantification of co-localisation between the fluorescence signals of overexpressed proteins, a minimum of 16 randomly chosen cells were analysed. Percentage co-localisation between respective sets of proteins is presented as mean values from at least three experiments ±SD. Co-localisation values were calculated by expressing the number of pixels in a given co-localisation mask as a percentage of total pixels for a given fluorophore. Co-localisation masks represent yellow pixels (overlapping green and red pixels) that have been extracted from the merged image. For quantitation of Golgi fragmentation due to siRNA treatments, 15 randomly selected fields containing a minimum of 16 cells were analysed per siRNA (Control or Rab30) over three independently performed experiments. Cells were scored on the basis of the distribution of GM130 displaying a dispersed or compact localisation.

Time-lapse microscopy

For time-lapse imaging, FRAP and FLIP experiments, HeLa cells were plated on 35-mm glass bottom culture dishes (MatTek) and transfected with the indicated GFP-fusion constructs. At 16–20 h after transfection, the culture dishes were mounted on a Heater Insert P (CarlZeiss), maintained at 37°C, and images were recorded at the indicated time intervals using a Zeiss LSM 510 META confocal microscope fitted with a 63 × 1.4 plan apochromat lens. For FRAP experiments, regions of interest (ROIs) were bleached at 100% laser power for 125 iterations and subsequent images were recorded at the indicated time intervals. For FLIP experiments, the ROI was bleached at 100% laser power for 125 iterations each minute for 7–9 min. For quantification of FRAP, the fluorescence recovery to the ROI was monitored for 350 s for five individual cells in each of three independently performed experiments. The data presented in the recovery curve represent the average fluorescence intensity ±SD for five recordings at 10 s intervals in three independently performed experiments. The data presented in the bar chart represent the mean ±SD of this data expressed as a percentage of total recovery to the ROI at 350 s. Time stamps were added using ImageJ.

Electron microscopy

For conventional EM, HeLa cells grown on coverslips were transfected with the indicated oligonucleotides as described. The cells were then fixed with 2.5% glutaraldehyde in 0.1 M cacodylate buffer for 24 h. After several washes with 0.1 M cacodylate buffer, the cells were post-fixed with reduced osmium for 45 min (2% OsO_4 and potassium ferrocyanide), dehydrated in ethanol, and embedded in Epon whilst on the coverslips. Ultrathin sections were counterstained with uranyl acetate before observation at the electron microscope. For ultrathin cryosectioning and immunogold labelling, cells were fixed with a mixture of 2% paraformaldehyde (PFA) and 0.2% glutaraldehyde in 0.1 M phosphate buffer, pH 7.4. Cells were processed for

ultracryomicrotomy and single- or double-immunogold labelled using protein A conjugated to 10 nm gold (PAG10) or 15 nm gold (PAG15) as reported previously (Giordano et al., 2009). Sections of resin embedded cells or immunogold labelled cryosections were observed under an electron microscope (FEI, CM120) equipped with a numeric camera KeenView (Soft Imaging System).

For quantification of Rab30 labelling, 300 gold particles (FLAG–Rab30) were counted and assigned to the compartment over which they were located in randomly selected profiles of cells in each of two experiments. The definition of the distinct compartments was based on their morphology and their previous characterisation by immunogold labelling with different organelle markers as reported by Giordano et al. (2009). Data are presented as a mean ±SD.

For evaluation of the Golgi phenotype, Golgi structures were counted in the same number of randomly selected Rab30-depleted or Control HeLa cells in each of two experiments. The results, expressed as percentage, are presented as a mean ±SD. The length of Golgi cisternae was measured in a total number of 30 Golgi structures from randomly acquired micrographs of siRab30- or siCtrl-treated cells by using the iTEM software (Intelligent Micrograph, Soft Imaging System) and was expressed in nanometres.

CTxB trafficking assay

HeLa cells were incubated for 30 min with complete DMEM supplemented with 4 μg/ml of Alexa Fluor-594 CTxB. Following this, cells were washed three times with PBS, incubated with fresh DMEM for the indicated chase time points and then processed for immunofluorescence microscopy.

VSV-G trafficking assay

HeLa cells were transfected with the indicated constructs. Six to 10 h after transfection, cells were transferred from a 37°C to 40°C incubator with a 5% CO_2 supply, for a further 10–12 h. Following this, the cells were either washed once briefly in PBS and then immediately fixed in 3% PFA or washed once, overlaid with complete DMEM supplemented with 50 μg/ml cycloheximide and transferred to a 32°C incubator for either 20 or 120 min. Cells were washed briefly after each time point, fixed in 3% PFA and processed for immunofluorescence microscopy as previously described (Horgan et al., 2005).

Author contributions

E.E.K. and F.G. designed and performed the experiments under the direction of M.W.M. and G.R., respectively. E.E.K. drafted the manuscript. All authors contributed to the interpretation of results, manuscript correction, finalisation and proofing.

Funding

This work was supported by Science Foundation Ireland grants (05/IN.3/B859, 08/RFP/NSC 1499 and 09/IN.1/B2629) to M.W.M. and by Institut Curie, Centre National de la Recherche Scientifique, Fondation pour la Recherche Médicale and Association pour la Recherche sur le Cancer to G.R.

Acknowledgements

The authors are deeply indebted to Sara Hanscom for her invaluable technical assistance and comments on the manuscript. We are grateful to George Banting for useful discussions during this study and to Jean Gruenberg for the anti-LBPA antibody. The authors are also grateful to Jeremy Simpson for useful discussions and for the very kind gifts of reagents. We would also like to thank Bruno Goud for providing the pGEX-2T/Rab30 plasmid construct.

Conflict of interest statement

The authors have declared no conflict of interest.

References

Allan, B.B., Moyer, B.D. and Balch, W.E. (2000) Rab1 recruitment of p115 into a *cis*-SNARE complex: Programming budding COPII vesicles for fusion. Science **289**, 444–448

Alvarez, C., Fujita, H., Hubbard, A. and Sztul, E. (1999) ER to Golgi transport: Requirement for p115 at a pre-Golgi VTC stage. J. Cell Biol. **147**, 1205–1222

Barr, F.A., Nakamura, N. and Warren, G. (1998) Mapping the interaction between GRASP65 and GM130, components of a protein complex involved in the stacking of Golgi cisternae. EMBO J. **17**, 3258–3268

Chen, D., Guo, J., Miki, T., Tachibana, M. and Gahl, W.A. (1996) Molecular cloning of two novel rab genes from human melanocytes. Gene **174**, 129–134

Chen, W., Feng, Y., Chen, D. and Wandinger-Ness, A. (1998) Rab11 is required for *trans*-golgi network-to-plasma membrane transport and a preferential target for GDP dissociation inhibitor. Mol. Biol. Cell **9**, 3241–3257

de Leeuw, H.P., Koster, P.M., Calafat, J., Janssen, H., van Zonneveld, A.J., van Mourik, J.A. and Voorberg, J. (1998) Small GTP-binding proteins in human endothelial cells. Br. J. Haematol. **103**, 15–19

Diao, A., Rahman, D., Pappin, D.J., Lucocq, J. and Lowe, M. (2003) The coiled-coil membrane protein golgin-84 is a novel rab effector required for Golgi ribbon formation. J. Cell Biol. **160**, 201–212

Giordano, F., Bonetti, C., Surace, E.M., Marigo, V. and Raposo, G. (2009) The ocular albinism type 1 (OA1) G-protein-coupled receptor functions with MART-1 at early stages of melanogenesis to control melanosome identity and composition. Hum. Mol. Genet. **18**, 4530–4545

Giordano, F., De Marzo, A., Vetrini, F. and Marigo, V. (2007) Fibroblast growth factor and epidermal growth factor differently affect differentiation of murine retinal stem cells *in vitro*. Mol. Vis. **13**, 1842–1850

Glick, B.S. and Malhotra, V. (1998) The curious status of the Golgi apparatus. Cell **95**, 883–889

Glick, B.S. and Nakano, A. (2009) Membrane traffic within the Golgi apparatus. Annu. Rev. Cell Dev. Biol. **25**, 113–132

Goud, B. and Gleeson, P.A. (2010) TGN golgins, Rabs and cytoskeleton: Regulating the Golgi trafficking highways. Trends Cell Biol. **20**, 329–336.

Grigoriev, I., Splinter, D., Keijzer, N., Wulf, P.S., Demmers, J., Ohtsuka, T., Modesti, M., Maly, I.V., Grosveld, F., Hoogenraad, C.C. and Akhmanova, A. (2007) Rab6 regulates transport and targeting of exocytotic carriers. Dev. Cell **13**, 305–314

Haas, A.K., Yoshimura, S., Stephens, D.J., Preisinger, C., Fuchs, E. and Barr, F.A. (2007) Analysis of GTPase-activating proteins: Rab1 and Rab43 are key Rabs required to maintain a functional Golgi complex in human cells. J. Cell Sci. **120**, 2997–3010

Horgan, C.P., Zurawski, T.H. and McCaffrey, M.W. (2005) Purification and functional properties of Rab11-FIP3. Methods Enzymol. **403**, 499–512

Huber, L.A., Pimplikar, S., Parton, R.G., Virta, H., Zerial, M. and Simons, K. (1993) Rab8, a small GTPase involved in vesicular traffic between the TGN and the basolateral plasma membrane. J. Cell Biol. **123**, 35–45

Janoueix-Lerosey, I., Jollivet, F., Camonis, J., Marche, P.N. and Goud, B. (1995) Two-hybrid system screen with the small GTP-binding protein Rab6. Identification of a novel mouse GDP dissociation inhibitor isoform and two other potential partners of Rab6. J. Biol. Chem. **270**, 14801–14808

Kelly, E.E., Horgan, C.P., Adams, C., Patzer, T.M., Ni Shuilleabhain, D.M., Norman, J.C. and McCaffrey, M.W. (2010) Class I Rab11-family interacting proteins are binding targets for the Rab14 GTPase. Biol. Cell **102**, 51–62

Kitt, K.N., Hernandez-Deviez, D., Ballantyne, S.D., Spiliotis, E.T., Casanova, J.E. and Wilson, J.M. (2008) Rab14 regulates apical targeting in polarized epithelial cells. Traffic **9**, 1218–1231

Klausner, R.D., Donaldson, J.G. and Lippincott-Schwartz, J. (1992) Brefeldin A: Insights into the control of membrane traffic and organelle structure. J. Cell Biol. **116**, 1071–1080

Klumperman, J., Schweizer, A., Clausen, H., Tang, B.L., Hong, W., Oorschot, V. and Hauri, H.P. (1998) The recycling pathway of protein ERGIC-53 and dynamics of the ER–Golgi intermediate compartment. J. Cell Sci. **111**, 3411–3425

Kondylis, V. and Rabouille, C. (2009) The Golgi apparatus: Lessons from Drosophila. FEBS Lett. **583**, 3827–3838

Lee, M.C., Miller, E.A., Goldberg, J., Orci, L. and Schekman, R. (2004) Bi-directional protein transport between the ER and Golgi. Annu. Rev. Cell Dev. Biol. **20**, 87–123

Lencer, W.I. and Tsai, B. (2003) The intracellular voyage of cholera toxin: Going retro. Trends Biochem. Sci. **28**, 639–645

Mardones, G.A., Snyder, C.M. and Howell, K.E. (2006) *Cis*-Golgi matrix proteins move directly to endoplasmic reticulum exit sites by association with tubules. Mol. Biol. Cell **17**, 525–538

Martinez, O., Antony, C., Pehau-Arnaudet, G., Berger, E.G., Salamero, J. and Goud, B. (1997) GTP-bound forms of rab6 induce the redistribution of Golgi proteins into the endoplasmic reticulum. Proc. Natl. Acad. Sci. U. S. A. **94**, 1828–1833

Matanis, T., Akhmanova, A., Wulf, P., Del Nery, E., Weide, T., Stepanova, T., Galjart, N., Grosveld, F., Goud, B., De Zeeuw, C.I., Barnekow, A. and Hoogenraad, C.C. (2002) Bicaudal-D regulates COPI-independent Golgi–ER transport by recruiting the dynein–dynactin motor complex. Nat. Cell Biol. **4**, 986–992

Monetta, P., Slavin, I., Romero, N. and Alvarez, C. (2007) Rab1b interacts with GBF1 and modulates both ARF1 dynamics and COPI association. Mol. Biol. Cell **18**, 2400–2410

Moyer, B.D., Allan, B.B. and Balch, W.E. (2001) Rab1 interaction with a GM130 effector complex regulates COPII vesicle *cis*-Golgi tethering. Traffic **2**, 268–276

Nilsson, T., Lucocq, J.M., Mackay, D. and Warren, G. (1991) The membrane spanning domain of beta-1,4-galactosyltransferase specifies trans Golgi localization. EMBO J. **10**, 3567–3575

Pelham, H.R. (1998) Getting through the Golgi complex. Trends Cell Biol. **8**, 45–49

Presley, J.F., Cole, N.B., Schroer, T.A., Hirschberg, K., Zaal, K.J. and Lippincott-Schwartz, J. (1997) ER-to-Golgi transport visualized in living cells. Nature **389**, 81–85

Puthenveedu, M.A., Bachert, C., Puri, S., Lanni, F. and Linstedt, A.D. (2006) GM130 and GRASP65-dependent lateral cisternal fusion allows uniform Golgi-enzyme distribution. Nat. Cell Biol. **8**, 238–248

Puthenveedu, M.A. and Linstedt, A.D. (2001) Evidence that Golgi structure depends on a p115 activity that is independent of the vesicle tether components giantin and GM130. J. Cell Biol. **155**, 227–238

Rogalski, A.A., Bergmann, J.E. and Singer, S.J. (1984) Effect of microtubule assembly status on the intracellular processing and surface expression of an integral protein of the plasma membrane. J. Cell Biol. **99**, 1101–1109

Sannerud, R., Saraste, J. and Goud, B. (2003) Retrograde traffic in the biosynthetic–secretory route: Pathways and machinery. Curr. Opin. Cell Biol. **15**, 438–445

Saraste, J. and Kuismanen, E. (1984) Pre- and post-Golgi vacuoles operate in the transport of Semliki Forest virus membrane glycoproteins to the cell surface. Cell **38**, 535–549

Shi, Z., Dragin, N., Miller, M.L., Stringer, K.F., Johansson, E., Chen, J., Uno, S., Gonzalez, F.J., Rubio, C.A. and Nebert, D.W. (2010) Oral benzo[a]pyrene-induced cancer: Two distinct types in different target organs depend on the mouse Cyp1 genotype. Int. J. Cancer **127**, 2334–2350

Short, B., Haas, A. and Barr, F.A. (2005) Golgins and GTPases, giving identity and structure to the Golgi apparatus. Biochim. Biophys. Acta. **1744**, 383–395

Short, B., Preisinger, C., Schaletzky, J., Kopajtich, R. and Barr, F.A. (2002) The Rab6 GTPase regulates recruitment of the dynactin complex to Golgi membranes. Curr. Biol. **12**, 1792–1795

Sinka, R., Gillingham, A.K., Kondylis, V. and Munro, S. (2008) Golgi coiled-coil proteins contain multiple binding sites for Rab family G proteins. J. Cell Biol. **183**, 607–615

Stenmark, H. (2009) Rab GTPases as coordinators of vesicle traffic. Nat. Rev. Mol. Cell. Biol. **10**, 513–525

Stenmark, H., Parton, R.G., Steele-Mortimer, O., Lutcke, A., Gruenberg, J. and Zerial, M. (1994) Inhibition of rab5 GTPase activity stimulates membrane fusion in endocytosis. EMBO J. **13**, 1287–1296

Storrie, B., White, J., Rottger, S., Stelzer, E.H., Suganuma, T. and Nilsson, T. (1998) Recycling of golgi-resident glycosyltransferases through the ER reveals a novel pathway and provides an explanation for nocodazole-induced Golgi scattering. J. Cell Biol. **143**, 1505–1521

Thomas, C., Rousset, R. and Noselli, S. (2009) JNK signalling influences intracellular trafficking during Drosophila morphogenesis through regulation of the novel target gene Rab30. Dev. Biol. **331**, 250–260

Tisdale, E.J., Bourne, J.R., Khosravi-Far, R., Der, C.J. and Balch, W.E. (1992) GTP-binding mutants of rab1 and rab2 are potent inhibitors of vesicular transport from the endoplasmic reticulum to the Golgi complex. J. Cell Biol. **119**, 749–761

White, J., Johannes, L., Mallard, F., Girod, A., Grill, S., Reinsch, S., Keller, P., Tzschaschel, B., Echard, A., Goud, B. and Stelzer, E.H. (1999) Rab6 coordinates a novel Golgi to ER retrograde transport pathway in live cells. J. Cell Biol., **147**, 743–760

Wilcke, M., Johannes, L., Galli, T., Mayau, V., Goud, B. and Salamero, J. (2000) Rab11 regulates the compartmentalization of early endosomes required for efficient transport from early endosomes to the *trans*-golgi network. J. Cell Biol. **151**, 1207–1220

Wilson, B.S., Nuoffer, C., Meinkoth, J.L., McCaffery, M., Feramisco, J.R., Balch, W.E. and Farquhar, M.G. (1994) A Rab1 mutant affecting guanine nucleotide exchange promotes disassembly of the Golgi apparatus. J. Cell Biol. **125**, 557–571

Received: 20 July 2011; Accepted: 24 November 2011; Accepted article online: 5 December 2011

